Scientific Research Publishing

Open Journal of Composite Materials, 2024, 14, 91-108
https://www.scirp.org/journal/ojcm
ISSN Online: 2164-5655
ISSN Print: 2164-5612

Study of Structural, Optical, Electrical and Dielectric Properties of Gd-Doped ZnO Composites Synthesized by Solid State Reaction Method

Santosh Kumar Kundara[1,2], Kanhaiya Chawla[1,3], Dinesh Kumar Yadav[1], Chhagan Lal[1], Balram Tripathi[4*], Narendra Jakhar[1*]

[1]Department of Physics, University of Rajasthan, Jaipur, India
[2]Sw. P.N.K.S. Government PG College, Dausa, India
[3]Government PG College, Pratapgarh, India
[4]S.S. Jain Subodh PG (Autonomous) College, Jaipur, India
Email: *balramtripathi1181@gmail.com, *jakharnaren@yahoo.com

How to cite this paper: Kundara, S.K., Chawla, K., Yadav, D.K., Lal, C., Tripathi, B. and Jakhar, N. (2024) Study of Structural, Optical, Electrical and Dielectric Properties of Gd-Doped ZnO Composites Synthesized by Solid State Reaction Method. *Open Journal of Composite Materials*, **14**, 91-108.
https://doi.org/10.4236/ojcm.2024.142007

Received: March 13, 2024
Accepted: April 27, 2024
Published: April 30, 2024

Abstract

In this manuscript, we are reporting structural, bonding, optical, dielectric, and electrical properties of Gd-doped ZnO composite samples ($Zn_{1-x}Gd_xO$, x = 0, 0.05, 0.10) prepared by solid-state reaction method. XRD spectra confirm the wurtzite hexagonal phase with a grain size distribution of 42 - 47 nm. The FT-IR spectra confirm bonding behavior like Zn-O, O=C=O, and O-H stretching modes. FESEM micrographs show that the grains of crystallites possess nearly spherical morphology. Optical absorption spectra confirm that the optical band gap decreases systematically from 3.19 eV to 3.15 eV for x = 0.0 to x = 0.10 samples. For all samples, PL spectra exhibited near-band emission, blue emission, and green emission peaks. The dielectric constant decreases as the applied frequency increases. Hall effect results show that with increasing doping concentration of Gd, mobility and resistivity increase while bulk concentration decreases. Current-Voltage study shows that current increases when temperature is increased. Rare earth-doped ZnO is potential material used for optoelectronics and spintronics device applications. Properties of Gd-doped ZnO are studied by various research groups, but dielectric studies are limitedly reported. Therefore, the present research work aims to study the change of electrical, optical, and dielectric properties of Gd-doped ZnO for device applications.

Keywords

ZnO:Gd Composites, Optical Band Gap, Green Emission, Dielectric

Constant

1. Introduction

In the past decades, the scientific and research interest in bulk and nanostructured wide-band semiconductors has grown. These materials have extraordinary properties like chemical, optical, dielectric, electrical and magnetic [1]. Among these semiconductors, pure zinc oxide has remarkable properties like wide bandgap (3.3 eV), and good optical transparency and furthermore, ZnO has an exciton binding energy of 60 meV, which is significantly greater than the thermal energy (25 meV) at ambient temperature. Additionally, inexpensive cost of manufacture, highly thermal stable, non-toxic, chemical and mechanical stable properties encourages the usage of ZnO in a variety of forms. Zinc oxide (ZnO) is one of the most essential metal oxides for the use in various forms like photocatalysts [2] [3], dye-sensitized solar cells [4], chemical sensors [5], spintronics [6], etc. Doping ZnO with suitable elements appears to increase its characteristics for device manufacturing. Transition metals like Co, Mn and Ni-doped ZnO have been widely investigated by various research groups [7] [8] [9] [10].

Doping ZnO with rare earth metals results in ferromagnetic characteristics [11]. Er-doped ZnO composites show room-temperature ferromagnetic characteristics [12]. The luminescence characteristics of Ce-doped ZnO nanocrystals demonstrate that the emission intensity is reduced, which is expected to be related to creating more surface defects [13]. ZnO:Nd^{3+} nanopowders were prepared by a controlled solid-state reaction method at high temperatures [14]. The presence of sharp visible emission in Nd-doped ZnO has enormous promise in light-emitting applications. Gd has been identified as a useful dopant among rare earth metals and has become the subject of numerous studies due to its intriguing applications in optoelectronic and magnetic devices. The addition of Gd (gadolinium) has drawn the interest of researchers due to the half-filled f-orbital influence, which is thought to have a significant impact on the photocatalytic activity of ZnO [2]. Gd doping in ZnO can be useful for energy harvesting devices [15]. Gd-doped ZnO thin films synthesized by sol-gel spin coating [16] and (Gd, Co) co-doped ZnO-based nanotubes synthesized by the co-precipitation method [17] can be used for spintronics applications. Solid state reaction method was used to synthesize ZnO phosphors co-doped with Gd^{3+}/Yb^{3+} [18]. Synthesized phosphors could be potentially used in light-emitting diodes. r-GO-supported Gd-doped ZnO composite prepared by the hydrothermal route is helpful in preparing an efficient photocatalyst [19]. Gd-doped ZnO thin films synthesized through the co-sputtering method show that the magnetic properties of ZnO increase after Gd doping, and the behavior of thin films changes from diamagnetic to paramagnetic after Gd doping [20].

Different synthesis techniques, like spray pyrolysis [21], sol-gel method [22],

magnetron sputtering [23], sonochemical methods [24], etc. are available for the synthesis of ZnO nanostructures with various morphology and size. Ma and Wang used a thermal evaporation vapor phase deposition process to synthesize Gd-doped ZnO nanocrystals [25]. Obeid *et al.* used the thermal decomposition method to prepare Gd-doped ZnO nanorods [26]. On the basis of application, several methods have been adopted for sample synthesis. The sample synthesized by solid-state reaction shows decreasing band gap of ZnO with increasing Gd concentration [27]. Yayapao *et al.* demonstrated that Gd-ZnO samples synthesized via the sonochemical method show better photocatalytic activity than undoped ZnO [28]. Gd-doped ZnO nanoparticles prepared by wet chemical method show that the band gap of ZnO decreases as the Gd doping concentration increases [29]. Gd-doped ZnO films were deposited by the RF magnetron sputtering technique, showing a hexagonal wurtzite structure. When Gd is doped, defect concentration increases, which results in enhanced deep-level emission [30]. Undoped and Gd-doped ZnO nanostructures synthesized by hydrothermal method show very high visible light luminescent properties, which make them potential materials for various device applications like sensors, LEDs, etc. [31]. Roy *et al.* studied structural, magnetic, and optical responses of Gd-doped ZnO nanoparticles synthesized by the co-precipitation technique and demonstrated that the synthesized samples show a lower band gap as compared to undoped ZnO [32].

The SSR method provides non-uniform atomic mixtures without using any chemical agents, acids, or any time-consuming chemical reactions. SSR method is the cheapest method of mixing as compared to all other available methods. No harmful chemicals are used in SSR method, so mixing with this method does not have any adverse effect on the environment. Here, we synthesized Gd-doped ZnO powder samples with varying dopant concentrations (x= 0, 0.05, 0.10) by solid-state reaction method. Structural, bonding, optical, dielectric, and electrical properties are investigated by X-ray diffraction (XRD), Fourier transform infrared (FTIR) spectroscopy, UV-Vis spectroscopy, Photoluminescence (PL) spectroscopy, Impedance analyzer, Hall measurement, and Current-voltage characteristics. Properties of ZnO could be tailored with the doping of rare earth metals. Among these rare earth metals, Gd doping shows effective results on the electrical, optical, dielectric, and magnetic properties of ZnO. To the authors' knowledge, the dielectric properties of the ZnO-Gd composite have not been extensively investigated. Therefore, in the present study, we present a systematic investigation of the electrical, optical, and dielectric properties of the ZnO-Gd composites.

2. Experimental Method

Solid state reaction was used to synthesize undoped ZnO and Gd-doped ZnO ($Zn_{1-X}Gd_XO$, x = 0.05, 0.10) composite samples. The starting materials, ZnO and Gd_2O_3, were weighed using an electronic balance to ensure proper stoichiometry.

These components were homogeneously mixed for sufficient time in a ball mill to produce fine powders and the resulting powders were calcined for 8 hours at 1000˚C in ambient circumstances. The mixture was ground for 1 hour after drying and further carried out for characterization. The structural properties of prepared powder samples were studied using XRD analysis. X-ray diffractometer model Panalytical X Pert Pro was used for measurement using Cu-K_α radiation (λ = 0.154 nm) in the 20˚ - 90˚ range. Step size of 0.03˚ and scan step time 0.60 s, were fixed for XRD analysis of undoped and Gd-doped ($Zn_{1-X}Gd_xO$, x = 0.05 and 0.10) samples. FTIR spectra were used to determine the chemical functional groups in synthesized samples using Bruker ALPHA spectrometer. The surface morphology of the synthesized samples was examined using a field emission scanning electron microscope (JEOL JSM-7610F Plus). Additionally, energy-dispersive X-ray analysis was performed to identify the chemical composition of the samples. Optical study of all the synthesized samples was done in the wavelength range of 350 - 550 nm through absorption spectra received from a UV-visible spectrophotometer (model-SHIMADZU UV-2600). To calculate the optical band gap of all prepared samples, Tauc's plot was used. Photoluminescence Spectroscopy was performed using a Horiba fluoroMax-4 spectrometer. Powder samples were pressed into pellets using a hydraulic press for dielectric constant measurements, and characterization was done using WAYNE KERR 6500B impedance analyzer instrument. Mobility, resistivity, and bulk concentration were calculated using the HMS-5000 series hall effect measurement system. The electrical properties of the synthesized samples were measured by MicroXact's SPS-2200 system IS premier manual probe station.

3. Result and Discussion

3.1. X-Ray Diffraction

X-ray diffraction was used to explore the formation of crystalline phases. **Figure 1** shows X-ray diffraction spectra of undoped ZnO and Gd-doped ZnO composite samples ($Zn_{1-X}Gd_XO$, x = 0.05 and 0.10) synthesized by solid-state reaction method. XRD data was collected within 2θ range of 20 - 90 degrees. The XRD pattern shows sharp, intense peaks compatible with the ZnO hexagonal wurtzite structure. In Gd-doped samples, additional peaks appeared at around 28.80 and 33.35 degrees, which are due to the occurrence of secondary phases of Gd_2O_3. With increasing Gd content, the intensity of diffraction peaks drops. This drop can be attributed to decreased crystallinity caused by crystallite size reduction and/or a difference in the ionic radius of dopant Gd^{3+} (0.93 Å) and host Zn^{2+} (0.74 Å) [33]. Compared to pure ZnO, the Gd-doped samples exhibit a shift towards a lower angle. Decreased intensities of peaks and shifting towards lower angles confirm that Gd is properly incorporated into the ZnO host lattice. The crystallite size of the synthesized samples was calculated using the Scherrer-equation given by [3]:

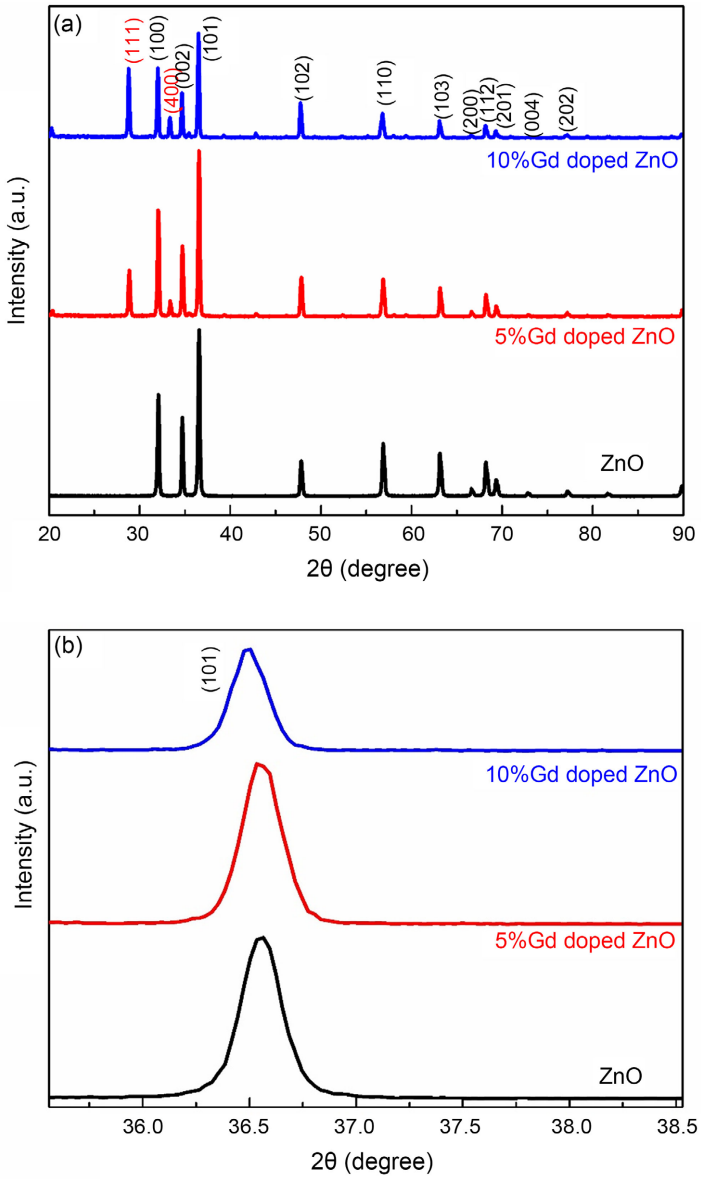

Figure 1. (a) XRD spectra of ZnO and $Zn_{1-X}Gd_xO$ (x = 0.05 and 0.10) samples; (b) Enlarged view of XRD pattern of (101) plane.

$$D = 0.89\lambda/\beta\cos\theta \quad (1)$$

In this equation, λ corresponds to the X-ray wavelength (1.5406 Å for Cu-Kα), β is the value of FWHM (full width at half maximum) in radian and θ is the Bragg diffraction angle. To calculate the average crystallite size (D) of as-prepared powder samples, the strongest peak (101) was selected. Results reveal that the average crystallite size (D) is in the 42 - 47 nm range and doped ZnO samples have smaller crystallite sizes than undoped ZnO samples, which are also in good agreement with earlier results [1] [3] [34] [35]. Gd doping in the ZnO host lattice played a crucial role in the crystallinity of synthesized samples. It was concluded that Gd doping affects the nucleation process and grain growth and by increasing Gd doping concentration, the increased cationic vacancies hinder the

nucleation process and grain growth which resulted in a reduction of crystallite size and shifting of the peaks towards lower 2θ angles and these results were also supported by earlier studies [35] [36] [37].

3.2. Morphological and Compositional Analysis

Figures 2(a)-(c) show the FESEM (field emission scanning electron microscopy) and EDX (energy dispersive X-ray analysis) images of pure, Gd-doped ZnO powder samples. These FESEM micrographs show that the grains of crystallites have a roughly spherical shape [1]. The grains stay together, resulting in a well-agglomeration of the crystallites. The development of bonds between nearby particles is the primary cause of agglomeration. The elemental compositions of the powder samples are confirmed by EDX. These spectra displayed the presence of Zn, O, and Gd in Gd-doped ZnO composite samples, whereas the spectrum of undoped ZnO shows the presence of only zinc and oxygen ions. The observed EDX result indicates the presence of Gd^{3+}, which has successfully substituted as a dopant in the ZnO matrix [35]. Particle size histogram derived from FESEM images revealed the average particle size and distribution. The obtained values of average particle size range from 156 nm to 202 nm, which could be the result of the aggregation of several tiny domains to create a particle [26] (**Figure 3**).

3.3. FTIR Analysis

Figure 4 shows the FT-IR spectra of undoped ZnO and Gd-doped ZnO ($Zn_{1-X}Gd_xO$, x = 0.05 and 0.10) composite samples.

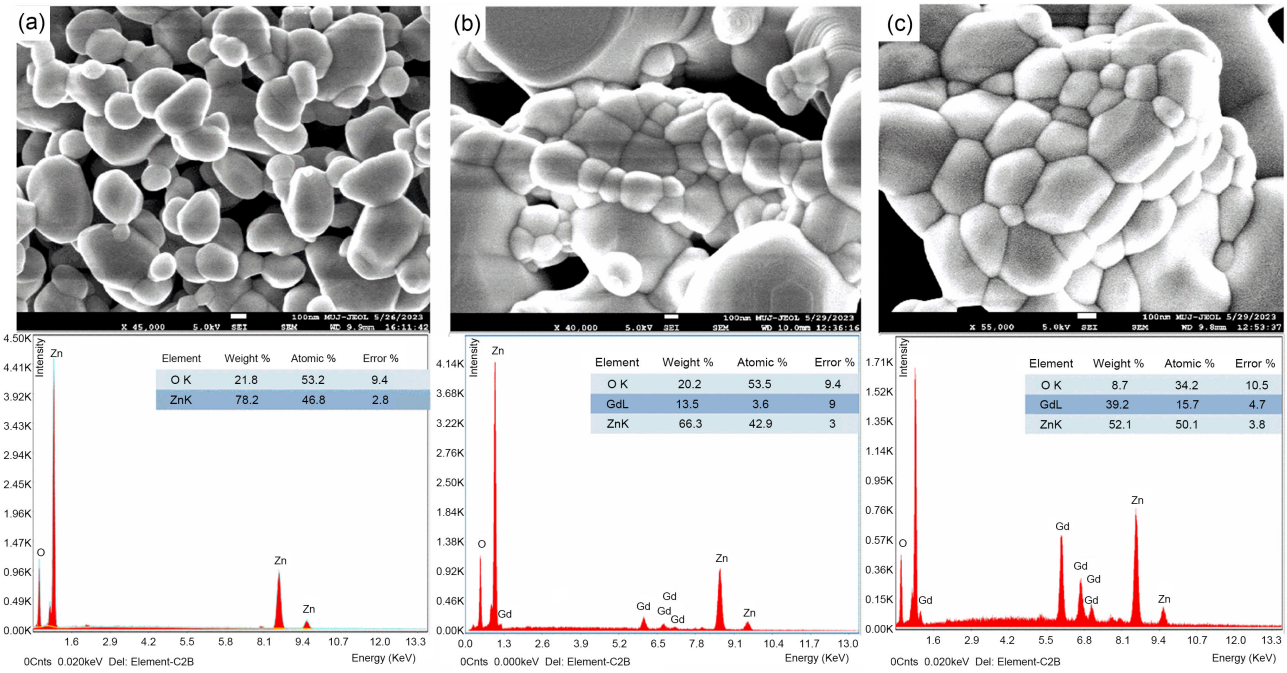

Figure 2. FESEM micrographs with EDX spectrum of (a) ZnO and ((b) (c)) $Zn_{1-x}Gd_xO$ (x = 0.05 and 0.10) samples.

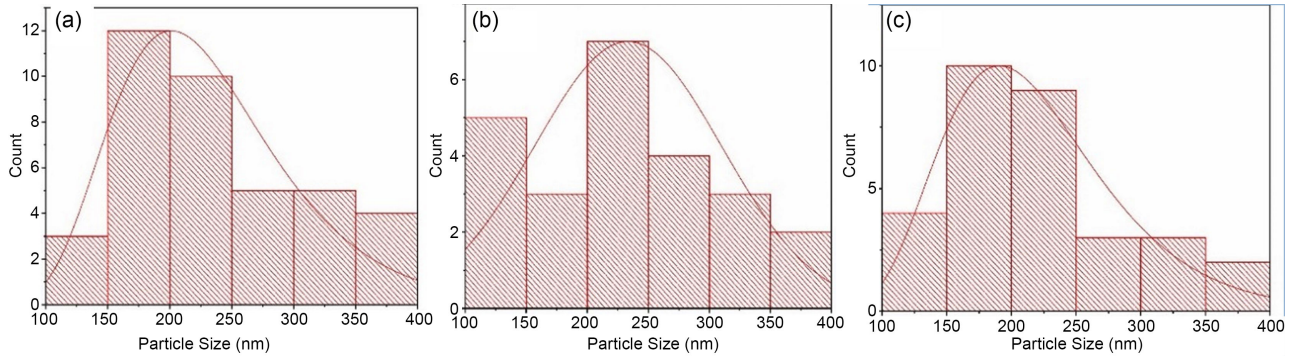

Figure 3. Particle size distribution histogram of (a) ZnO and (b, c) $Zn_{1-x}Gd_xO$ (x = 0.05 and 0.10) samples.

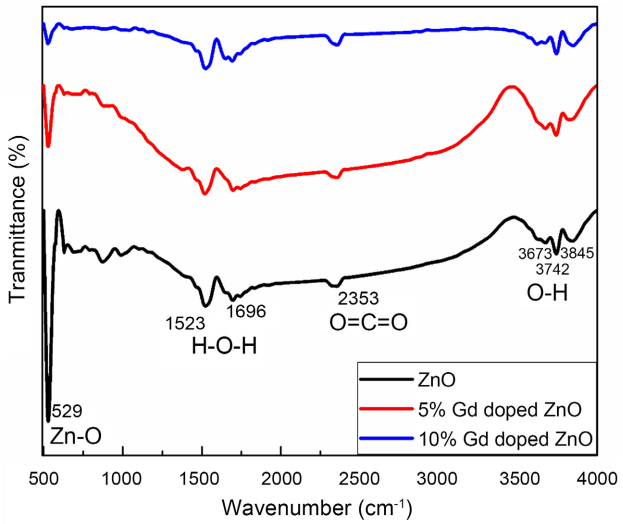

Figure 4. FTIR spectrum of ZnO and $Zn_{1-x}Gd_xO$ (x = 0.05 and 0.10) samples.

In order to find out functional groups in undoped ZnO and Gd-doped ZnO powder samples, FTIR study was done in the range of 500 - 4000 cm^{-1}. The characteristic absorption band of ZnO appears at low wavenumbers [38] [39]. In our findings, it appeared near 529 cm^{-1} which corresponds to the stretching vibration mode of the ZnO bond. The intensity of the Zn-O stretching peaks in Gd-doped ZnO samples has decreased because Zn^{2+} ions are substituted by the Gd^{3+} dopants in the lattice of Gd-doped ZnO [40]. The peak appearing near 2353 cm^{-1} is assigned to the O=C=O, which is adsorbed on the surface during the FTIR process [2] [3] [41]. Since the composite samples were processed in the ambient atmosphere, it is possible that some water molecules came from the air as well. The absorption bands around 3673 - 3845 cm^{-1} correspond to O-H stretching vibration, which is nearly good agreement with earlier reports [3] [42] [43]. The absorption band around 1523 - 1696 cm^{-1} appears due to water molecules that are adsorbed on the surface of ZnO [42].

3.4. Optical Analysis

Figure 5(a) shows the absorption spectra of pure ZnO and Gd-doped ZnO

($Zn_{1-X}Gd_xO$, x = 0.05 and 0.10) composite samples in the wavelength range from 350 - 550 nm. The absorbance of these samples depends upon many factors like the size of particles, Oxygen deficiency, the roughness of surface, etc. **Figure 5(a)** shows that the position of the absorption edge shifts towards a higher wavelength side when Gd is doped in ZnO powder samples. The optical bandgap values of all the synthesized samples were calculated using Tauc's plot, and these were found to be 3.19 eV, 3.16 eV, and 3.15 eV for undoped ZnO and Gd-doped ZnO samples respectively. Doped samples have lower band gap as comparison to undoped samples and these results were also earlier reported [1] [22] [44]. Gd doping creates new electronic levels or subbands within the ZnO band gap. These new electronic levels or subbands combine with the conduction band, which results in the continuous band and further reduction in the band gap [22] [45].

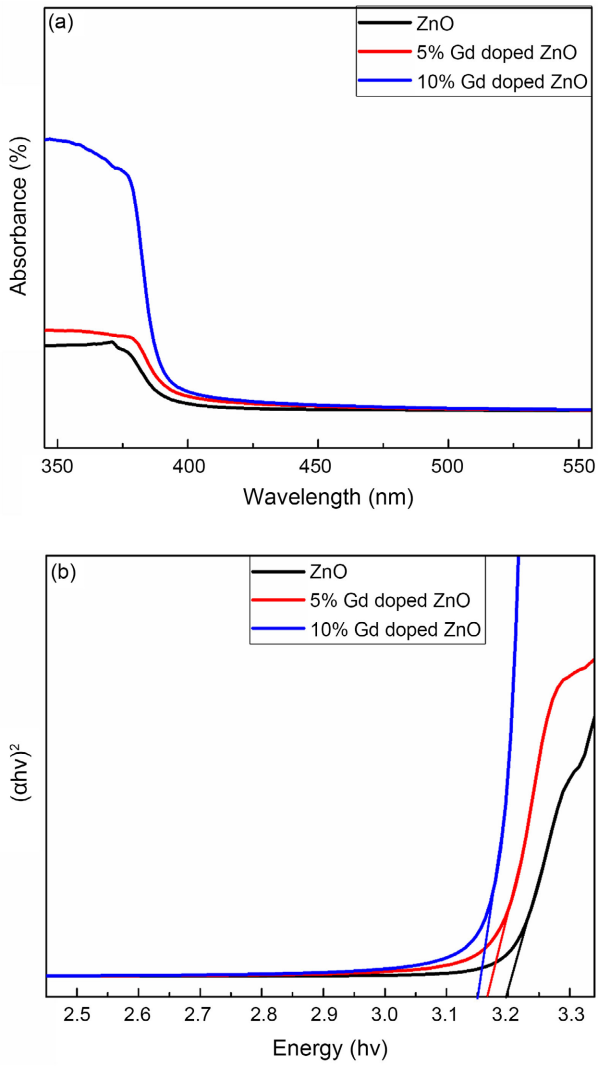

Figure 5. (a) Absorption spectra for ZnO and $Zn_{1-X}Gd_xO$ (x = 0.05 and 0.10) samples; (b) Optical band gap for ZnO and $Zn_{1-X}Gd_xO$ (x = 0.05 and 0.10) samples.

3.5. Photoluminescence Study

The photoluminescence (PL) spectra of pure ZnO and Gd-doped ZnO powder samples at room temperature are presented in **Figure 6**. The Photoluminescence analysis of pure ZnO and Gd-doped ZnO powder samples were performed at a wavelength of 350 nm. **Figure 6** shows that the prepared samples have three emission bands: 1) violet emission is represented by a peak centered near 420 nm, 2) peaks centered near 457 nm correspond to blue emission and 3) peaks centered near 497 nm represent the green emission. Violet emission near 420 nm is caused by a transition between conduction band and zinc vacancy related acceptor levels [36] [46]. In all samples, the electronic transition between zinc interstitial (Zn_i) and zinc vacancy (V_{Zn}) levels induces blue emission near 457 nm [36] [37] [47] [48]. Green emission, which occurs near 497 nm, is attributed to an electron transition caused by the defect level in the band gap in all samples. Oxygen vacancies or zinc interstitials could be the possible defects [37] [39] [49]. The PL results indicate that the samples contain many microstructural defects, which will undoubtedly help the doped ZnO samples to regulate their electrical properties.

3.6. Dielectric Studies

Figure 7 depicts the dielectric constant's changes with frequency measured at room temperature.

In nanostructure materials, various processes like electronic, ionic, dipolar, and space charge polarization, etc. play important roles in the dielectric behavior of the materials. The value of the dielectric constant of the synthesized samples was calculated using the formula:

$$\varepsilon' = Cd/\varepsilon_0 A$$

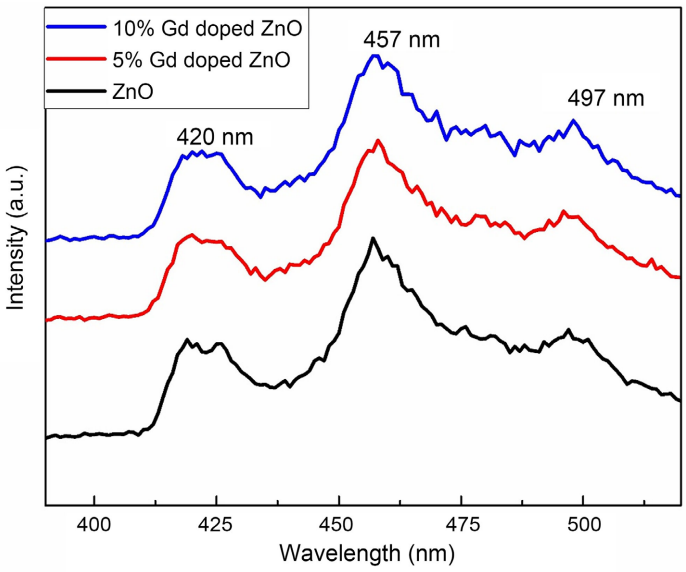

Figure 6. Photoluminescence spectra of ZnO and $Zn_{1-X}Gd_xO$ (x = 0.05 and 0.10) samples.

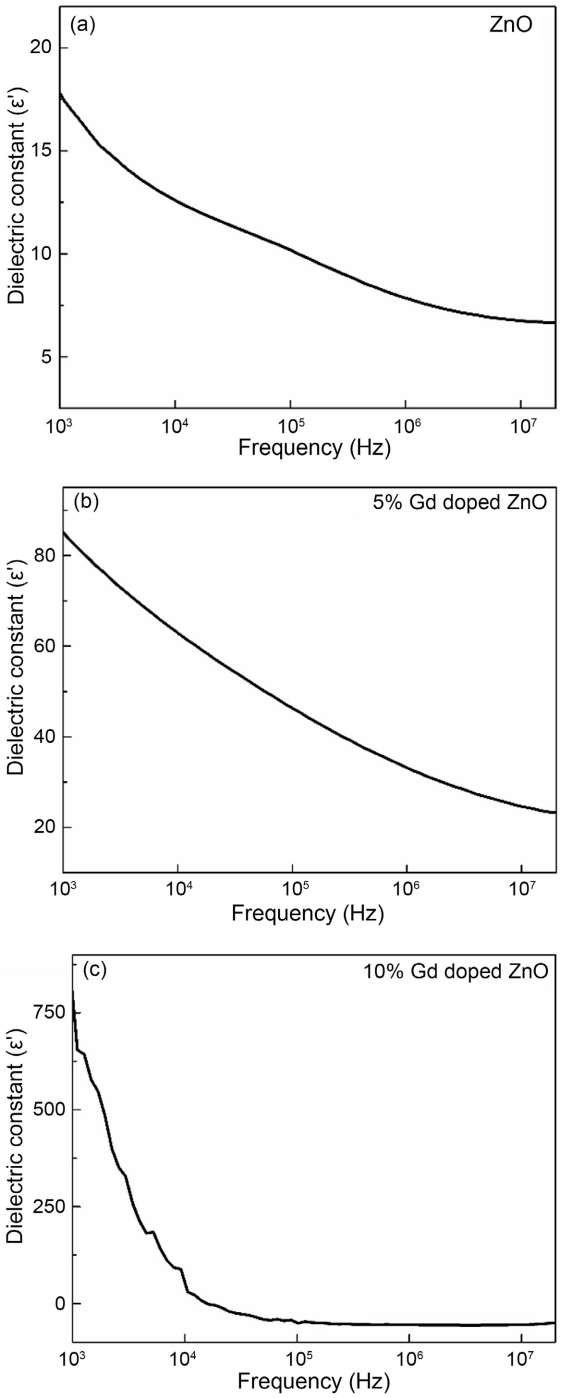

Figure 7. Dielectric constant of (a) ZnO and ((b) (c)) $Zn_{1-X}Gd_xO$ (x = 0.05 and 0.10) samples.

where ε_0, C are the free space permittivity and capacitance of the sample respectively. d and A are the thickness and area of the pellet. The dielectric constant (ε') of the undoped ZnO and Gd-doped samples decreases as the frequency of the applied electric field increases. This result can be explained using the Maxwell-Wagner model, which suggests that well-conducted grains are separated by poorly conducted grain borders in a dielectric structure. It is explained in earlier

reports also [35] [36] [37]. By hopping, due to high resistance electrons can accumulate at grain boundaries and produce polarization. Furthermore, Permanent dipoles can align in the direction of an externally applied electric field at low frequencies, contributing to dielectric characteristics. As the frequency of the external electric field increases, the hopping frequency of electrons cannot follow it. Due to this, electrons cannot reach the grain boundary, and as a result, polarization decreases. The findings of this study and the explanation mentioned above are consistent with the Koops phenomenological theory [50]. It is observed in many studies that the dielectric constant decreases when Gd is doped in the ZnO crystal lattice. Franco Jr. *et al.* reported the same outcome [45], but in our study, dielectric constants increased after Gd doping in ZnO. Possible explanation for this result is the presence of several interfacial polarizations within the material [36].

3.7. Hall Measurement

The variation in Bulk concentration, Hall mobility, resistivity, and conductivity as a function of different Gd concentrations is shown in **Figure 8** and **Figure 9**. The bulk concentration decreases while the mobility and resistivity increase with Gd doping. An increase in grain boundary defects that act as free carrier traps could explain the drop in bulk concentration. The Hall mobility and resistivity depend mainly on charge carrier scattering. The most common scattering centers include ionized impurities, crystal defects, phonons, and grain boundaries. Therefore, the influence of ionized impurities on the scattering process may result in greater Hall mobility and resistivity. Similar results were reported with other rare earth metals like Er and Yb-doped ZnO [51].

3.8. Current-Voltage (I-V) Characteristics

Figure 10 shows the current-voltage characteristics of undoped ZnO and Gd-doped

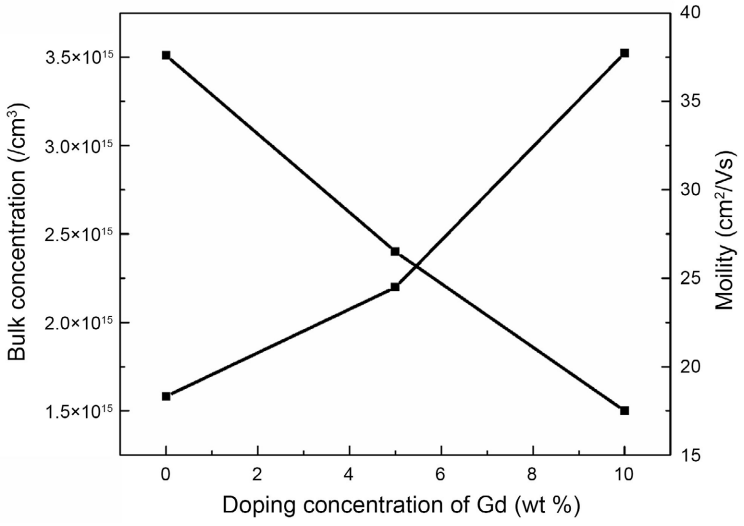

Figure 8. Variation in bulk concentration and hall mobility as a function of different Gd concentrations.

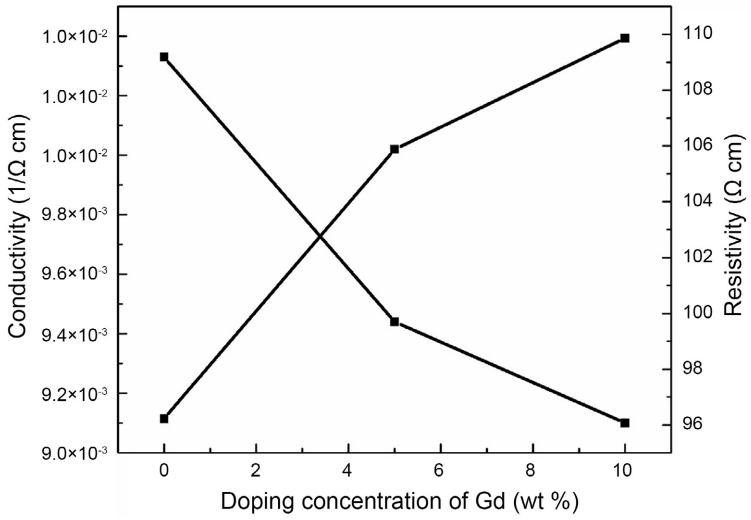

Figure 9. Variation in conductivity and resistivity as a function of different Gd concentrations.

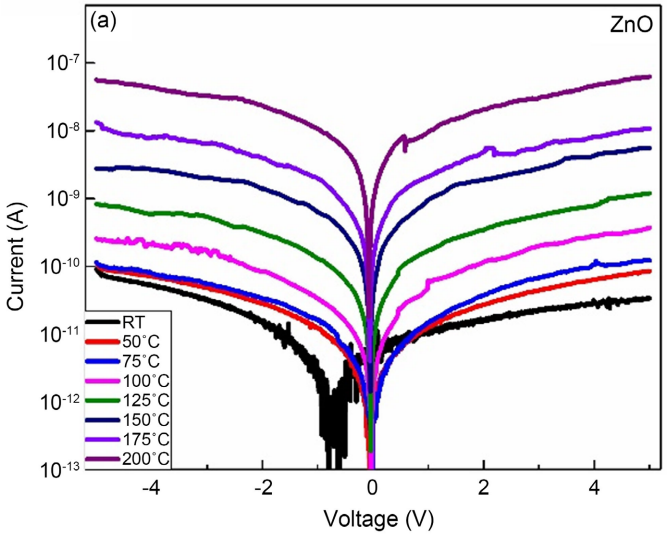

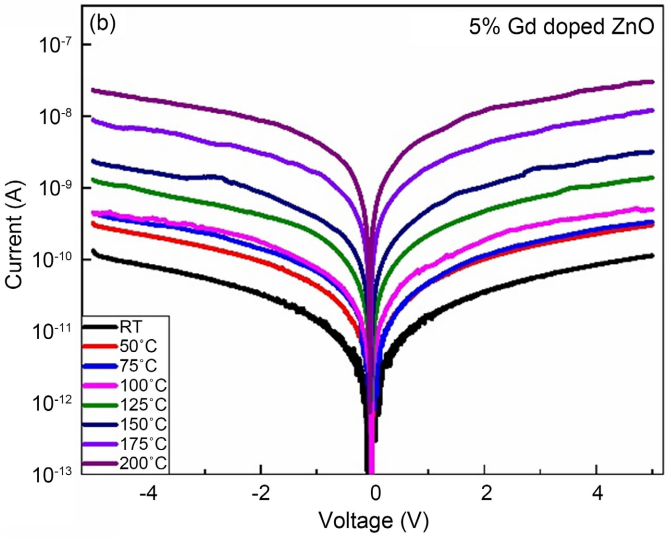

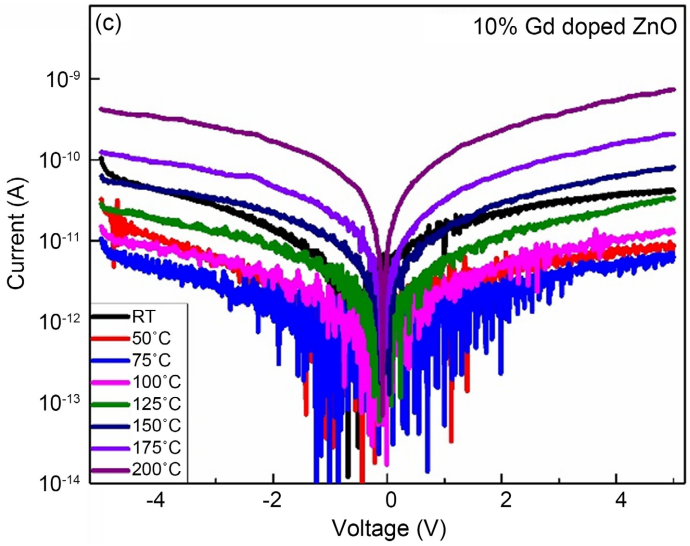

Figure 10. Current-voltage characteristics of (a) ZnO and ((b) (c)) $Zn_{1-X}Gd_xO$ (x = 0.05 and 0.10) samples.

ZnO powder samples from room temperature to 200˚C. Results show that when Gd doping is increased, current decreases. It could be predicted that the scattering process becomes more effective when the doping percentage of Gd is increased, due to which resistance is increased. It is also observed that with increasing temperature, current increases in undoped ZnO and 5% Gd-doped ZnO samples. In the 10% Gd-doped ZnO sample, initially, the current decreases with increasing temperature, and later, it starts to increase with temperature.

4. Conclusion

In summary, Gd-doped ZnO ($Zn_{1-x}Gd_xO$, where x = 0, 0.05, 0.10) composite samples were prepared using the solid-state reaction method. The structural analysis confirms a wurtzite hexagonal-type structure with a grain size distribution of 42 - 47 nm. Ball milling reduces the grain size and provides atomic-level mixing, thereby increasing the active surface area of ZnO-Gd composites. The larger active surface area is most responsible for the improvement in electrical, optical, and dielectric properties of the ZnO-Gd composites. FTIR analysis shows the existence of various chemical functional groups like Zn-O, O=C=O and O-H in the synthesized samples. FESEM micrographs show that the grains of crystallites possess nearly spherical morphology and they stay together, resulting in a well-agglomeration. Optical absorption spectra show the variation in the optical band gap between 3.19 eV to 3.15 eV. PL studies show that undoped and Gd-doped ZnO samples exhibit near-band, blue, and deep-level emission peaks. Dielectric studies show a higher value of the dielectric constant of Gd-doped ZnO powder samples. Due to these high dielectric values, it could be a promising choice for charge storage applications. Hall effect results show that with increasing doping concentration of Gd, mobility and resistivity increase while bulk concentration decreases. Current-Voltage characteristics show current decreases when dop-

ing is increased from 0% to 10%. ZnO-Gd composites have a high dielectric constant, which can be used in charge storing devices, in transformer, it can be used as an insulator and as a cooling agent. The mixture has a high active surface area, which can be used in high-performance solar cells, gas sensors, etc.

Conflicts of Interest

The authors declare no conflicts of interest regarding the publication of this paper.

References

[1] Punia, K., Lal, G., Dalela, S., Dolia, S.N., Alvi, P.A., Barbar, S.K., Modi, K.B. and Kumar, S. (2021) A Comprehensive Study on the Impact of Gd Substitution on Structural, Optical and Magnetic Properties of ZnO Nanocrystals. *Journal of Alloys and Compounds*, **868**, Article ID: 159142. https://doi.org/10.1016/j.jallcom.2021.159142

[2] Selvaraj, S., Mohan, M.K., Navaneethan, M., Ponnusamy, S. and Muthamizhchelvan, C. (2019) Synthesis and Photocatalytic Activity of Gd Doped ZnO Nanoparticles for Enhanced Degradation of Methylene Blue under Visible Light. *Materials Science in Semiconductor Processing*, **103**, Article ID: 104622. https://doi.org/10.1016/j.mssp.2019.104622

[3] Ghouri, M.I., Ahmed, E., Khalid, N.R., Ahmad, M., Ramzan, M., Shakoor, A. and Niaz, N.A. (2014) Gadolinium Doped ZnO Nanocrystalline Powders and Its Photocatalytic Performance for Degradation of Methyl Blue under Sunlight. *Journal of Ovonic Research*, **10**, 89-100.

[4] Umar, A., Singh, P., Al-Ghamdi, A.A. and Al-Heniti, S. (2010) Direct Growth of ZnO Nanosheets on FTO Substrate for Dye-Sensitized Solar Cells Applications. *Journal of Nanoscience and Nanotechnology*, **10**, 6666-6671. https://doi.org/10.1166/jnn.2010.3294

[5] Weißenrieder, K.S. and Müller, J. (1997) Conductivity Model for Sputtered ZnO-Thin Film Gas Sensors. *Thin Solid Films*, **300**, 30-41. https://doi.org/10.1016/S0040-6090(96)09471-0

[6] Ronning, C., Gao, P.X., Ding, Y., Wang, Z.L. and Schwen, D. (2004) Manganese-Doped ZnO Nanobelts for Spintronics. *Applied Physics Letters*, **84**, 783-785. https://doi.org/10.1063/1.1645319

[7] Singhal, R.K., Jakhar, N., Samariya, A., Dolia, S.N. and Kumar, S. (2018) Effect of Co and O Defects on Ferromagnetism in Co-Doped ZnO: An X-Ray Absorption Spectroscopic Investigation. *Physica B*: *Condensed Matter*, **530**, 1-6. https://doi.org/10.1016/j.physb.2017.10.094

[8] Jakhar, N., Samariya, A., Sharma, S.C., Dhawan, M., Palsania, H.S., Dolia, S.N. and Singhal, R.K. (2017) X-Ray Absorption Spectroscopic Investigation of Ferromagnetic Ni-Doped ZnO. *Macromolecular Symposia*, **376**, Article ID: 1700054. https://doi.org/10.1002/masy.201700054

[9] Kundara, S.K., Verma, M.K., Bidiyasar, R., Chawla, K., Lal, N., Lal, C., Akhtar, M.S., *et al.* (2023) Tailoring the Structural, Optical and Electrical Properties of Mn Doped ZnO Thin Films for Gas Sensing Response. *Science of Advanced Materials*, **15**, 772-780. https://doi.org/10.1166/sam.2023.4475

[10] Singhal, R.K., Sharma, S.C. and Jakhar, N. (2011) XPS Study of Some Dilute Magnetic Semiconductors. *AIP Conference Proceedings*, **1391**, 62-64.

https://doi.org/10.1063/1.3646780

[11] Dakhel, A.A. and El-Hilo, M. (2010) Ferromagnetic Nanocrystalline Gd-Doped ZnO Powder Synthesized by Coprecipitation. *Journal of Applied Physics*, **107**, Article ID: 123905. https://doi.org/10.1063/1.3448026

[12] John, R. and Rajakumari, R. (2012) Synthesis and Characterization of Rare Earth Ion Doped Nano ZnO. *Nano-Micro Letters*, **4**, 65-72.

[13] George, A., Sharma, S.K., Chawla, S., Malik, M.M. and Qureshi, M.S. (2011) Detailed of X-Ray Diffraction and Photoluminescence Studies of Ce Doped ZnO Nanocrystals. *Journal of Alloys and Compounds*, **509**, 5942-5946. https://doi.org/10.1016/j.jallcom.2011.03.017

[14] Jayanthi, K., Manorama, S.V. and Chawla, S. (2013) Observation of Nd^{3+} Visible Line Emission in ZnO:Nd^{3+} Prepared by a Controlled Reaction in the Solid State. *Journal of Physics D*: *Applied Physics*, **46**, Article ID: 325101. https://doi.org/10.1088/0022-3727/46/32/325101

[15] Goel, S., Sinha, N., Yadav, H., Godara, S., Joseph, A.J. and Kumar, B. (2017) Ferroelectric Gd-Doped ZnO Nanostructures: Enhanced Dielectric, Ferroelectric and Piezoelectric Properties. *Materials Chemistry and Physics*, **202**, 56-64. https://doi.org/10.1016/j.matchemphys.2017.08.067

[16] Ani, N.C., Sahdan, M.Z., Nayan, N., Adriyanto, F. and Wibowo, K.M. (2022) Investigation of Spin Polarization in Gd-Doped ZnO Films for High-Performance Organic Spintronic Devices. *Materials Science and Engineering B*, **276**, Article ID: 115536.https://doi.org/10.1016/j.mseb.2021.115536

[17] Khan, R., Shigidi, I., Al Otaibi, S., Althubeiti, K., Abdullaev, S.S., Rahman, N., Khan, A., *et al.* (2022) Room Temperature Dilute Magnetic Semiconductor Response in (Gd, Co) Co-Doped ZnO for Efficient Spintronics Applications. *RSC Advances*, **12**, 36126-36137. https://doi.org/10.1039/D2RA06637H

[18] Chakraborty, M., Banerjee, D., Singh, S. and Dutta, J. (2023) Photoluminescence and EPR Investigation in ZnO:Gd^{3+}, Yb^{3+} Phosphors for Application in Light Emitting Diode. *Materials Science in Semiconductor Processing*, **166**, Article ID: 107758. https://doi.org/10.1016/j.mssp.2023.107758

[19] Palanivel, B., Hossain, M.S., Macadangdang Jr, R.R., Dhas, S.S.J., Al-Enizi, A.M., Ubaidullah, M., Arockiam, S.I., *et al.* (2023) Effect of RGO Support on Gd@ZnO for UV-Visible-Light Driven Photocatalytic Organic Pollutant Degradation. *Journal of Rare Earths*, **41**, 1525-1531. https://doi.org/10.1016/j.jre.2022.07.019

[20] Raship, N.A., Tawil, S.N.M. and Nayan, N. (2024) Enhanced Magnetic Properties of Gd-Doped ZnO by Varying the Gd Concentration via Co-Sputtering Technique. *Materials Science Forum*, **1114**, 15-20. https://doi.org/10.4028/p-RXb3gr

[21] Rouchdi, M., Salmani, E., Fares, B., Hassanain, N. and Mzerd, A. (2017) Synthesis and Characteristics of Mg Doped ZnO Thin Films: Experimental and *Ab-Initio* Study. *Results in Physics*, **7**, 620-627. https://doi.org/10.1016/j.rinp.2017.01.023

[22] Aggarwal, N., Kaur, K., Vasishth, A. and Verma, N.K. (2016) Structural, Optical and Magnetic Properties of Gadolinium-Doped ZnO Nanoparticles. *Journal of Materials Science*: *Materials in Electronics*, **27**, 13006-13011. https://doi.org/10.1007/s10854-016-5440-2

[23] Chen, H., Ding, J., Shi, F., Li, Y. and Guo, W. (2012) Optical Properties of Ti-Doped ZnO Films Synthesized via Magnetron Sputtering. *Journal of Alloys and Compounds*, **534**, 59-63. https://doi.org/10.1016/j.jallcom.2012.04.064

[24] Phuruangrat, A., Yayapao, O., Thongtem, T. and Thongtem, S. (2014) Synthesis and Characterization of Europium-Doped Zinc Oxide Photocatalyst. *Journal of Nanoma-*

terials, **2014**, Article ID: 367529. https://doi.org/10.1155/2014/367529

[25] Ma, X. and Wang, Z. (2012) The Optical Properties of Rare Earth Gd Doped ZnO Nanocrystals. *Materials Science in Semiconductor Processing*, **15**, 227-231. https://doi.org/10.1016/j.mssp.2011.05.013

[26] Obeid, M.M., Jappor, H.R., Al-Marzoki, K., Al-Hydary, I.A., Edrees, S.J. and Shukur, M.M. (2019) Unraveling the Effect of Gd Doping on the Structural, Optical, and Magnetic Properties of ZnO Based Diluted Magnetic Semiconductor Nanorods. *RSC Advances*, **9**, 33207-33221. https://doi.org/10.1039/C9RA04750F

[27] Gora, M.K., Kumar, A., Choudhary, B.L., Dolia, S.N., Kumar, S. and Singhal, R.K. (2023) Electronic, Structural and Optical Properties of Gd-Doped ZnO Powder Synthesized by Solid-State Reaction Method. *Bangladesh Journal of Scientific and Industrial Research*, **58**, 53-64. https://doi.org/10.3329/bjsir.v58i1.63634

[28] Yayapao, O., Thongtem, T., Phuruangrat, A. and Thongtem, S. (2015) Synthesis and Characterization of Highly Efficient Gd Doped ZnO Photocatalyst Irradiated with Ultraviolet and Visible Radiations. *Materials Science in Semiconductor Processing*, **39**, 786-792. https://doi.org/10.1016/j.mssp.2015.06.039

[29] Sahu, D., Panda, N.R. and Acharya, B.S. (2017) Effect of Gd Doping on Structure and Photoluminescence Properties of ZnO Nanocrystals. *Materials Research Express*, **4**, Article ID: 114001. https://doi.org/10.1088/2053-1591/aa9597

[30] Yi, X.Y., Ma, C.Y., Yuan, F., Wang, N., Qin, F.W., Hu, B.C. and Zhang, Q.Y. (2017) Structural, Morphological, Photoluminescence and Photocatalytic Properties of Gd-Doped ZnO Films. *Thin Solid Films*, **636**, 339-345. https://doi.org/10.1016/j.tsf.2017.05.020

[31] Malik, K.A., Malik, J.H., Bhat, A.A., Assadullah, I. and Tomar, R. (2021) Trap Assisted Visible Light Luminescent Properties of Hydrothermally Grown Gd Doped ZnO Nanostructures. *Vacuum*, **183**, Article ID: 109832. https://doi.org/10.1016/j.vacuum.2020.109832

[32] Roy, S., Ghosh, M.P., Mohanty, S. and Mukherjee, S. (2022) Effects of Gd Ions Doping on the Microstructural, Magnetic and Optical Properties in ZnO Nanocrystals. *Bulletin of Materials Science*, **45**, Article No. 193. https://doi.org/10.1007/s12034-022-02766-6

[33] Sambasivam, S., Joseph, D.P., Asiri Naidu, S., Hui, K.N., Hui, K.S. and Choi, B.C. (2015) Intense Violet-Blue Emission and Paramagnetism of Nanocrystalline Gd^{3+} Doped ZnO Ceramics. *Journal of Advanced Ceramics*, **4**, 300-306. https://doi.org/10.1007/s40145-015-0164-y

[34] Khajuria, H., Ladol, J., Singh, R., Khajuria, S. and Sheikh, H.N. (2015) Surfactant Assisted Sonochemical Synthesis and Characterization of Gadolinium Doped Zinc Oxide Nanoparticles. *Acta Chimica Slovenica*, **62**, 849-858. https://doi.org/10.17344/acsi.2015.1558

[35] Aparna, P.U., Divya, N.K. and Pradyumnan, P.P. (2016) Structural and Dielectric Studies of Gd Doped ZnO Nanocrystals at Room Temperature. *Journal of Materials Science and Chemical Engineering*, **4**, 79-88. https://doi.org/10.4236/msce.2016.42009

[36] Das, S., Das, S., Roychowdhury, A., Das, D. and Sutradhar, S. (2017) Effect of Gd Doping Concentration and Sintering Temperature on Structural, Optical, Dielectric and Magnetic Properties of Hydrothermally Synthesized ZnO Nanostructure. *Journal of Alloys and Compounds*, **708**, 231-246. https://doi.org/10.1016/j.jallcom.2017.02.216

[37] Das, S., Das, S. and Sutradhar, S. (2017) Effect of Gd^{3+} and Al^{3+} on Optical and Di-

electric Properties of ZnO Nanoparticle Prepared by Two-Step Hydrothermal Method. *Ceramics International*, **43**, 6932-6941.
https://doi.org/10.1016/j.ceramint.2017.02.116

[38] Ibrahim, A.A., Hwang, S.W., Dar, G.N., Kim, S.H., Abaker, M. and Ansari, S.G. (2015) Synthesis and Characterization of Gd-Doped ZnO Nanopencils for Acetone Sensing Application. *Science of Advanced Materials*, **7**, 1241-1246.
https://doi.org/10.1166/sam.2015.2016

[39] Vijayaprasath, G., Murugan, R., Hayakawa, Y. and Ravi, G. (2016) Optical and Magnetic Studies on Gd Doped ZnO Nanoparticles Synthesized by Co-Precipitation Method. *Journal of Luminescence*, **178**, 375-383.
https://doi.org/10.1016/j.jlumin.2016.06.004

[40] Khataee, A., Soltani, R.D.C., Karimi, A. and Joo, S.W. (2015) Sonocatalytic Degradation of a Textile Dye Over Gd-Doped ZnO Nanoparticles Synthesized through Sonochemical Process. *Ultrasonics Sonochemistry*, **23**, 219-230.
https://doi.org/10.1016/j.ultsonch.2014.08.023

[41] Gawai, U.P., Patil, A.R., Sonawane, T.B., Huse, V.R. and Bodke, M.R. (2019) Influence of Gd Substitutionon Different Properties of ZnO Nanoparticles. *IOSR Journal of Engineering* (*IOSRJEN*), **9**, 51-57.

[42] Oprea, O., Vasile, O.R., Voicu, G., Craciun, L. and Andronescu, E. (2012) Photoluminescence, Magnetic Properties and Photocatalytic Activity of Gd^{3+} Doped ZnO Nanoparticles. *Digest Journal of Nanomaterials & Biostructures* (*DJNB*), **7**, 1757-1766.

[43] Dhir, R. (2020) Photocatalytic Degradation of Methyl Orange Dye under UV Irradiation in the Presence of Synthesized PVP Capped Pure and Gadolinium Doped ZnO Nanoparticles. *Chemical Physics Letters*, **746**, Article ID: 137302.
https://doi.org/10.1016/j.cplett.2020.137302

[44] Bharathi, P., Mohan, M.K., Shalini, V., Harish, S., Navaneethan, M., Archana, J., Hayakawa, Y., *et al.* (2020) Growth and Influence of Gd Doping on ZnO Nanostructures for Enhanced Optical, Structural Properties and Gas Sensing Applications. *Applied Surface Science*, **499**, Article ID: 143857.
https://doi.org/10.1016/j.apsusc.2019.143857

[45] Franco Jr., A. and Pessoni, H.V.S. (2017) Effect of Gd Doping on the Structural, Optical Band-Gap, Dielectric and Magnetic Properties of ZnO Nanoparticles. *Physica B: Condensed Matter*, **506**, 145-151.
https://doi.org/10.1016/j.physb.2016.11.011

[46] Venkatesh, P.S., Purushothaman, V., Muthu, S.E., Arumugam, S., Ramakrishnan, V., Jeganathan, K. and Ramamurthi, K. (2012) Role of Point Defects on the Enhancement of Room Temperature Ferromagnetism in ZnO Nanorods. *CrystEngComm*, **14**, 4713-4718. https://doi.org/10.1039/c2ce25098e

[47] Wei, X., Man, B., Xue, C., Chen, C. and Liu, M. (2006) Blue Luminescent Center and Ultraviolet-Emission Dependence of ZnO Films Prepared by Pulsed Laser Deposition. *Japanese Journal of Applied Physics*, **45**, Article No. 8586.
https://doi.org/10.1143/JJAP.45.8586

[48] Zeng, H., Duan, G., Li, Y., Yang, S., Xu, X. and Cai, W. (2010) Blue Luminescence of ZnO Nanoparticles Based on Non-Equilibrium Processes: Defect Origins and Emission Controls. *Advanced Functional Materials*, **20**, 561-572.
https://doi.org/10.1002/adfm.200901884

[49] Gong, Y., andelman, T., Neumark, G.F., O'Brien, S. and Kuskovsky, I.L. (2007) Origin of Defect-Related Green Emission from ZnO Nanoparticles: Effect of Surface Modification. *Nanoscale Research Letters*, **2**, Article No. 297.

https://doi.org/10.1007/s11671-007-9064-6

[50] Koops, C.G. (1951) On the Dispersion of Resistivity and Dielectric Constant of Some Semiconductors at Audio Frequencies. *Physical Review*, **83**, 121-124. https://doi.org/10.1103/PhysRev.83.121

[51] Senol, S.D. (2016) Hydrothermal Derived Nanostructure Rare Earth (Er, Yb)-Doped ZnO: Structural, Optical and Electrical Properties. *Journal of Materials Science: Materials in Electronics*, **27**, 7767-7775. https://doi.org/10.1007/s10854-016-4765-1